Porphyrinic Dyads and Triads Assembled around Iridium(III) Bis-terpyridine: Photoinduced Electron Transfer Processes

Isabelle M. Dixon,[§] Jean-Paul Collin,*[,§] Jean-Pierre Sauvage,*[,§] and Lucia Flamigni*[,‡]

Laboratoire de Chimie Organo-Minérale, UMR 7513 CNRS, Université Louis Pasteur, Institut Le Bel, 4, rue Blaise Pascal, 67070 Strasbourg, France, and Istituto FRAE-CNR, Via P. Gobetti 101, 40129 Bologna, Italy

Received April 17, 2001

Multicomponent arrays based on a central iridium(III) bis-terpyridine complex (**Ir**) used as assembling metal and free-base, zinc(II) or gold(III) tetraaryl-porphyrins (**PH_2**, **PZn**, **PAu**) have been designed to generate intramolecular photoinduced charge separation. The rigid dyads **PH_2−Ir**, **PZn−Ir**, **PAu−Ir**, and the rigid and linear triads **PH_2−Ir−PAu**, **PZn−Ir−PAu**, as well as the individual components **Ir**, **PH_2**, **PZn**, **PAu** have been synthesized and characterized by various techniques including electrochemistry. Their photophysical properties either in acetonitrile or in dichloromethane and toluene have been determined by steady-state and time-resolved methods. In acetonitrile, excitation of the triad **PH_2−Ir−PAu** leads to a charge separation with an efficiency of 0.5 and a resulting charge-separated (CS) state with a lifetime of 3.5 ns. A low-lying triplet localized on PH_2 and the presence of the heavy Ir(III) ion offer the CS state an alternative deactivation path through the triplet state. The behavior of the triad **PZn−Ir−PAu** in dichloromethane is rather different from that of **PH_2−Ir−PAu** in acetonitrile since the primary electron transfer to yield **PZn^+−Ir^-−PAu** is not followed by a secondary electron transfer. In this solvent, both unfavorable thermodynamic and electronic parameters contribute to the inefficiency of the second electron-transfer reaction. In contrast, in toluene solutions, the triad **PZn−Ir−PAu** attains a CS state with a unitary yield and a lifetime of 450 ns. These differences can be understood in terms of ground-state charge-transfer interactions as well as different stabilization of the intermediate and final CS states by solvent.

Introduction

Artificial photosynthesis has been a very active area of research for more than 3 decades, with the elaboration and study of models of natural systems or of synthetic devices aimed at converting light energy into chemical or electrical energy. An important source of inspiration has been the disclosure of the structure of bacterial photosynthetic Reaction Centers (RC).[1] In the past 20 years, many light-triggered charge separation molecular systems have been designed to mimick the processes taking place in the RC.[2] Porphyrins have been used as components of such devices since the very beginning, due to their resemblance with natural components and due to the fact that the redox and spectroscopic properties of these chromophores can be widely varied by the use of electroactive or bulky substituents and by their coordination to different transition metals.[3]

In the models elaborated by the Strasbourg group in the course of the past decade, a free-base or zinc(II) porphyrin is used as chromophore and primary electron donor, while a gold(III)-metalated porphyrin serves as electron acceptor.[4] In a modular strategy,[5] the electro-active components are assembled around an octahedral transition metal complex of the bis-terpyridine type, allowing the construction of linear triads with fixed intercomponent distances. Ruthenium(II) bis-terpyridine is a well-known complex[6] which can act as electron relay between two porphyrins.[7] A detailed photophysical study on the systems based on Ru(II) bis-terpyridine has evidenced that the presence of a relatively low-lying excited-state allows parasitic energy transfer to take place between the chromophore in its excited state and the central metal complex.[8] Therefore ruthenium has to be replaced by another transition metal in order to prevent the undesired energy transfer.

An iridium(III) bis-terpyridine unit was selected on the basis of its photophysical[9,10] and electrochemical properties,[10] and on

* To whom correspondence should be sent. E-mail: sauvage@chimie.u-strasbg.fr; flamigni@frae.bo.cnr.it.

§ Université Louis Pasteur.

‡ Istituto FRAE-CNR.

(1) Deisenhofer, J.; Epp, O.; Miki, K.; Huber, R.; Michel, H. *Nature* **1985**, *318*, 618. Deisenhofer, J.; Michel, H. *EMBO J.* **1989**, *8*, 2149. Huber, R. *Angew. Chem., Int. Ed. Engl.* **1989**, *101*, 849; *28*, 848.

(2) Gust, D.; Moore, T. A.; Moore, A. L. *Acc. Chem. Res.* **1993**, *26*, 198 and references therein. Wasielewski, M. R. *Chem. Rev.* **1992**, *92*, 435 and references therein. Kurreck, H.; Huber, M. *Angew. Chem., Int. Ed. Engl.* **1995**, *107*, 929; *34*, 849. Osuka, A.; Nakajima, S.; Okada, T.; Taniguchi, S.; Nozaki, K.; Ohno, T.; Yamazaki, I.; Nishimura, Y.; Mataga, N. *Angew. Chem., Int. Ed. Engl.* **1996**, *108*, 98; *35*, 92. Imahori, H.; Yamada, K.; Hasegawa, M.; Taniguchi, S.; Okada, T.; Sakata, Y. *Angew. Chem., Int. Ed. Engl.* **1997**, *109*, 2740; *36*, 2626. Wiederrecht, G. P.; Niemczyk, M. P.; Svec, W. A.; Wasielewski, M. R. *J. Am. Chem. Soc.* **1996**, *118*, 81 and references therein.

(3) *The porphyrin handbook*; Kadish, K. M.; Smith, K. M., Guilard, R. Eds, Academic Press, 2000.

(4) Heitz, V.; Chardon-Noblat, S.; Sauvage, J.-P. *Tetrahedron Lett.* **1991**, *32*, 197.

(5) Harriman, A.; Sauvage, J.-P. *Chem. Soc. Rev.* **1996**, 41.

(6) Maestri, M.; Armaroli, N.;. Balzani, V.; Constable, E. C.; Cargill Thompson, A. M. W. *Inorg. Chem.* **1995**, *34*, 2759. Sauvage, J.-P.; Collin, J.-P.; Chambron, J.-C.; Guillerez, S.; Coudret, C.; Balzani, V.; Barigelletti, F.; De Cola, L.; Flamigni, L. *Chem. Rev.* **1994**, *94*, 993. Collin, J.-P.; Gaviña, P.; Heitz, V.; Sauvage, J.-P. *Eur. J. Inorg. Chem.* **1998**, 1.

(7) Harriman, A.; Odobel, F.; Sauvage, J.-P. *J. Am. Chem. Soc.* **1995**, *117*, 9461.

(8) (a) Flamigni, L.; Barigelletti, F.; Armaroli, N.; Collin, J.-P.; Sauvage, J.-P.; Williams, J. A. G. *Chem. Eur. J.* **1998**, *4*, 1744. (b) Flamigni, L.; Barigelletti, F.; Armaroli, N.; Ventura, B.; Collin, J.-P.; Sauvage, J.-P.; Williams, J. A. G. *Inorg. Chem.* **1999**, *38*, 661.

(9) Ayala, N. P.; Flynn, C. M., Jr.; Sacksteder, L. A.; Demas, J. N.; DeGraff, B. A. *J. Am. Chem. Soc.* **1990**, *112*, 3837.

10.1021/ic010416t CCC: $20.00
Published on Web 09/06/2001

Chart 1. Structures of the Arrays and of the Models[a]

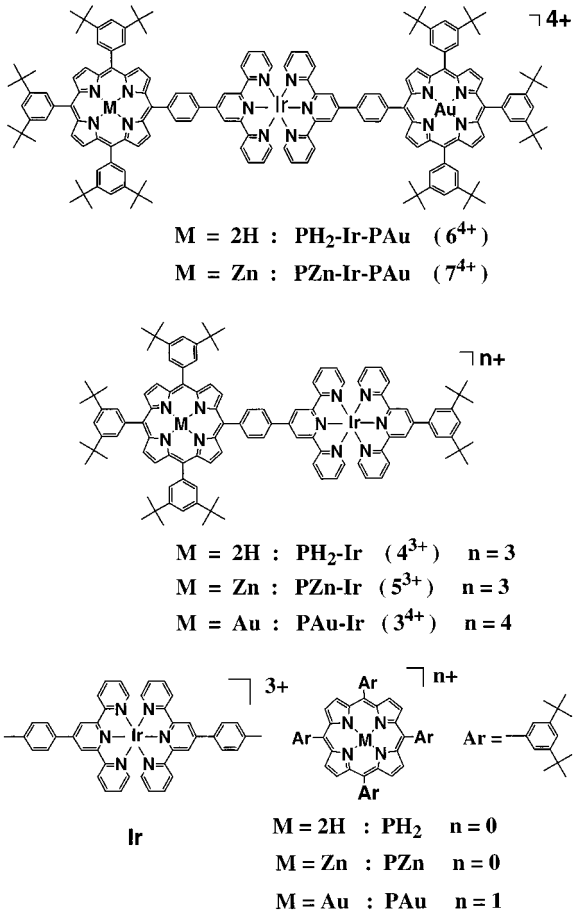

[a] Some of the compounds have a double nomenclature, the numbers being used in the synthetic part.

the basis of what one can expect from a third-row transition metal, in terms of the kinetic inertness of the coordination sphere which allows the construction of unsymmetrical arrays. Iridium(III) polyimine complexes have highly energetic excited states[11] which avoid the risk of energy transfer from a porphyrinic component, and a relatively good ability to accept electrons. Following relatively mild reaction conditions developed recently,[10] porphyrinic triads **PH$_2$−Ir−PAu** and **PZn−Ir−PAu**[12] were synthesized. The schematic structures of the triads and relevant dyads and reference compounds are represented in Chart 1. Their synthesis and the photophysical studies either in acetonitrile or in dichloromethane and toluene will be reported in this paper.

Results and Discussion

Design and Synthetic Strategy. Chart 2 summarizes (a) the principle of photoinduced electron tranfer processes in the triads and (b) the strategy used in their synthesis.

The unsymmetrical porphyrin **1** (Chart 3) illustrates the strong point of the modular approach employed here: once the ligand **1** is available in sufficient quantity, the dyads and triads are obtained by playing in the right order with the coordination chemistry of zinc(II), iridium(III) and gold(III).

Chart 2[a]

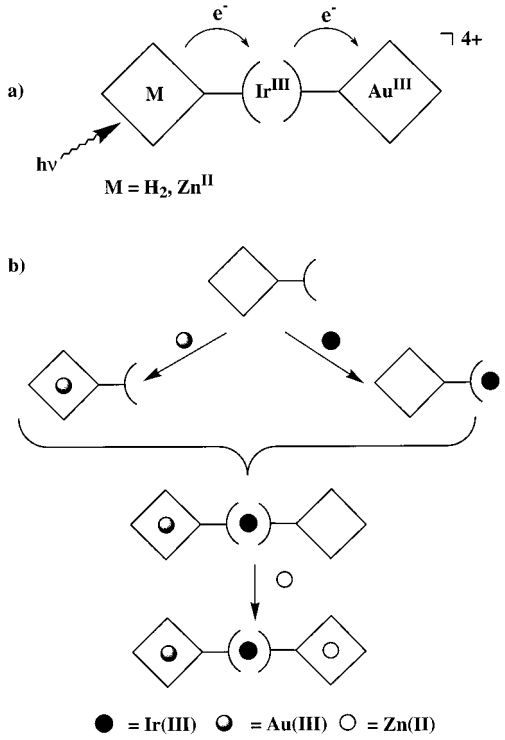

[a] The lozenges are porphyrins and the arcs of circle represent terpyridine coordinating sites.

The unsymmetrical porphyrin **1** bearing one terpy substituent was prepared following a Suzuki coupling procedure between a porphyrin bearing a boronic ester (**9**) and 4′-bromo-2,2′:6′,2″-terpyridine (Br-terpy).[13] Selective and quantitative protection of the boronic acid site of 4-formylphenylboronic acid with 2,2-dimethylpropane-1,3-diol gave the corresponding boronic ester **8** in quantitative yield. This boronic ester bearing an aldehydic function was used in the synthesis of porphyrin **9** under Lindsey's conditions.[14] It was reacted with pyrrole and 3,5-ditertiobutylbenzaldehyde[15] in chloroform for 1 h, under Lewis-acid catalysis by boron trifluoride etherate (Chart 3). The hereafter formed porphyrinogen was irreversibly oxidized by chloranil. The isolated yield of the mono-boronic porphyrin (A_3B) was limited to 4% by the difficulty to separate it by column chromatography from the trans bis (boronic) porphyrin (A_2B_2), identified by ^{1}H NMR. This is due to their very similar polarities and molecular weights. However is it possible to make the Suzuki coupling with Br-terpy on this mixture of A_3B and A_2B_2-types porphyrins, respectively forming the mono- and bis-terpy substituted porphyrins, which are easier to separate. Doing this, we evaluated the yield of formation of A_3B porphyrin to about 10%, which is usual for a statistical synthesis of unsymmetrical porphyrins.

A Suzuki coupling[16] reaction of porphyrin **9** with Br-terpy in the presence of sodium carbonate and palladium tetrakis-triphenylphosphine allowed the formation of terpy-substituted porphyrin **1**. It was isolated by chromatography on alumina in 79% yield.

(10) Collin, J.-P.; Dixon, I. M.; Sauvage, J.-P.; Williams, J. A. G.; Barigelletti, F.; Flamigni, L. *J. Am. Chem. Soc.* **1999**, *121*, 5009.
(11) Dixon, I. M.; Collin, J.-P.; Sauvage, J.-P.; Flamigni, L.; Encinas, S.; Barigelletti, F. *Chem. Soc. Rev.* **2000**, *29*, 385.
(12) Dixon, I. M.; Collin, J.-P.; Sauvage, J.-P.; Barigelletti, F.; Flamigni, L. *Angew. Chem., Int. Ed.* **2000**, *39*, 1292; Flamigni, L, Dixon, I. M., Collin, J.-P. Sauvage J.-P. *J. Chem. Soc. Chem. Commun.* **2000**, 2479.
(13) Whittle, B.; Batten, S. R.; Jeffery, J. C.; Rees, L. H.; Ward, M. D. *J Chem. Soc., Dalton Trans.* **1996**, 4249.
(14) Lee, C.-H.; Lindsey, J. S. *Tetrahedron* **1994**, *50*, 11427.
(15) Newman, M. S.; Lee, L. F. *J. Org. Chem.* **1972**, *37*, 4448.
(16) Miyaura, N.; Yanagi, T.; Suzuki, A. *Synth. Comm.* **1981**, *11*, 513.

Chart 3

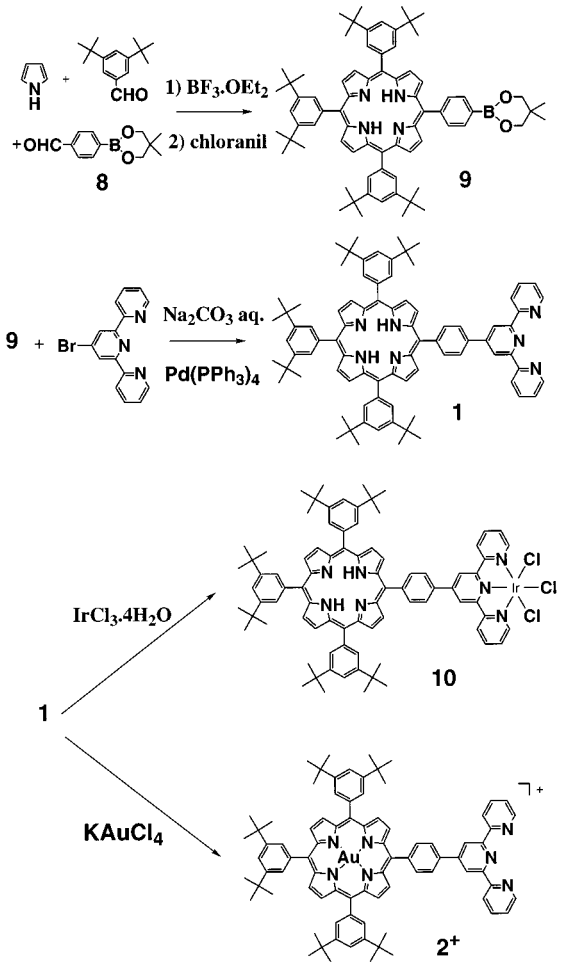

Metalation of **1** with gold(III) was achieved by reaction of the free-base porphyrin and potassium tetrachloroaurate to give the corresponding Au^{III} porphyrin $\mathbf{2}^{+}$ in 89% yield.[17] (Chart 3).

The gold(III) dyad $\mathbf{3}^{4+}$ was prepared by reaction of porphyrin $\mathbf{2}^{+}$ with previously prepared Ir(Ar-terpy)Cl_3,[10] by heating them in ethylene glycol under argon for 3 h at 140 °C. $\mathbf{3}^{4+}$ was isolated in 96% yield after chromatography on silica gel (Chart 4).

In the case of the free-base or zinc porphyrin, the first coordination of iridium was achieved on the porphyrin-substituted terpy itself. The trichloride precursor **10** was obtained in 58% isolated yield following the conditions developed for highly soluble terpys,[10] i.e., by reaction of porphyrin **1** with $IrCl_3 \cdot 4H_2O$ in refluxing ethanol for 2h30. It is remarkable that metalation is highly selective: Au(III) reacts with the porphyrin site only whereas Ir(III) leads exclusively to the terpy complex. The free-base dyad $\mathbf{4}^{3+}$ was prepared by reacting precursor **10** with Ar-tpy in refluxing ethylene glycol under argon for 25 min, and was isolated in 66% yield on a 40-mg scale. The free-base triad $\mathbf{6}^{4+}$ (Chart 4) was obtained by reaction of the same precursor **10** with gold(III) porphyrin $\mathbf{2}^{+}$ in refluxing ethylene glycol under argon for 25 min.

$\mathbf{6}^{4+}$ was isolated on the same scale as the dyad in 33% yield, as well as the bis-gold **PAu**−**Ir**−**PAu** array. The zinc series was obtained by metalation of the free-base dyad and triad to give the zinc dyad **PZn**−**Ir** and the zinc triad **PZn**−**Ir**−**PAu** in 80−100% yield.

Chart 4

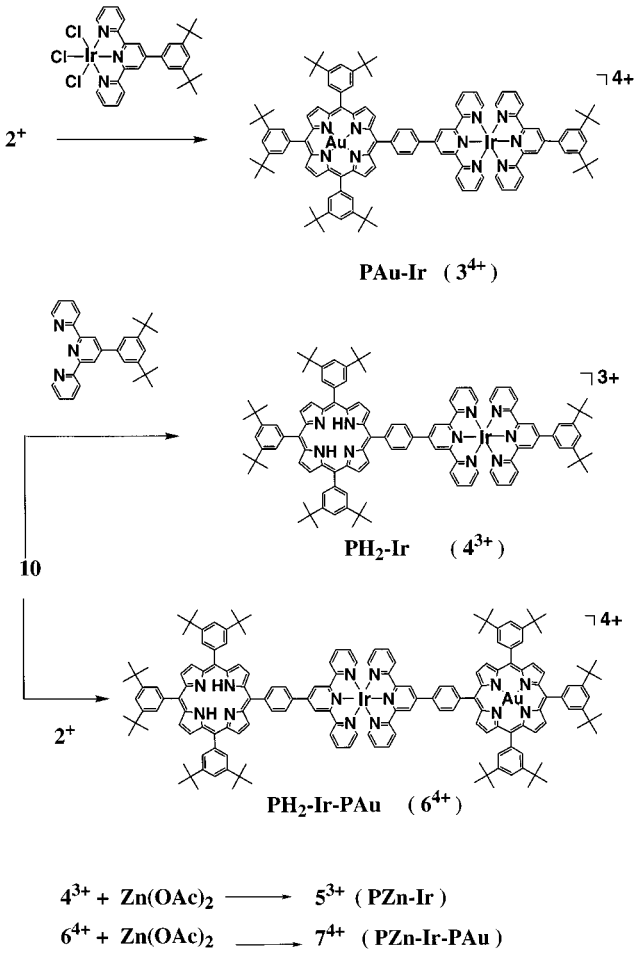

Table 1. Cyclic Voltammetry Data of the Dyads and Reference Compounds in CH_3CN and CH_2Cl_2

	$E^{ox}_{1/2}$ (V vs SCE)			$E^{red}_{1/2}$ (V vs SCE)		
	P^{2+}/P^{+}	P^{+}/P	terpy/terpy^{-}	terpy^{-}/terpy^{2-}	P/P^{-}	P^{-}/P^{2-}
			CH_3CN			
Ir			−0.78	−0.94		
PAu					−0.63	−1.02
PH_2−**Ir**		0.96	−0.78	−0.94	−1.17	
PZn−**Ir**	0.95	0.62 (irr)	−0.79	−0.95		
PAu−**Ir**			−0.75	−0.91	−0.59	−1.11
			CH_2Cl_2			
PH_2		0.86			−1.28	
PZn	1.09	0.68				
PAu					−0.70	−1.23
PH_2−**Ir**		0.88	−0.72	−0.88	−1.24	
PZn−**Ir**	1.08	0.68	−0.71	−0.87		
PAu−**Ir**			−0.72	−0.87	−0.66	

Electrochemistry

The redox characteristics of the dyads **PH_2**−**Ir**, **PAu**−**Ir**, **PZn**−**Ir**, and the reference compounds **Ir**, **PAu**, **PH_2**, and **PZn** (see Chart 1) examined by cyclic voltammetry in CH_3CN and CH_2Cl_2 are reported in Table 1. Due to the insolubility of the reference compounds **PH_2** and **PZn** in CH_3CN their redox potentials are given only in CH_2Cl_2. Monoelectronic waves observed for all redox processes were easily assigned to their individual components. As in the case of similar dyads involving tetraarylporphyrin and Rh(III) terpyridine complexes[18] the redox

(17) Jamin, M. E.; Iwamoto, R. T. *Inorg. Chim. Acta* **1978**, *27*, 135.

(18) Odobel, F. Thesis, Strasbourg, 1994.

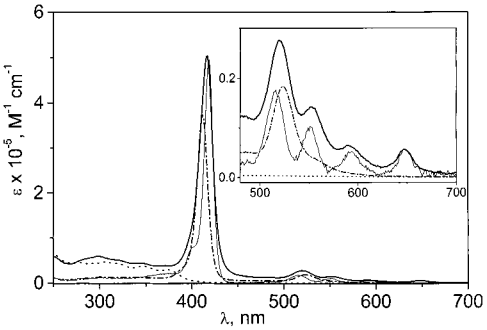

Figure 1. Molar absorption coefficients of the models PH_2 (—), **Ir** (···), **PAu** (-·-·-), and of the triad PH_2**−Ir−PAu** (—) in acetonitrile solutions. In the inset the region of the porphyrin Q-bands is expanded.

Table 2. Luminescence Properties and Energy Levels of the Excited States of PH_2**−Ir−PAu** and Models in Nitriles[a]

		298 K			77 K		
	state	λ_{max} (nm)	τ (ns)	Φ_{fluo}	λ_{max} (nm)	τ (μs)	E (eV)[b]
Ir[c]	^{3}Ir	506	2400[d]	0.029[d]	494	39	2.51
PH_2[e]	$^1PH_2$	652	8.3	0.15[f]	647	0.011	1.92
	$^3PH_2$				840[f]	6000[f]	1.47[f]
PAu[g]	^{3}PAu				710	10; 100	1.75
PH_2**−Ir**[e]	$^1PH_2$	652	0.03	0.002	648	0.012	1.91
PAu−Ir[g]	^{3}PAu				705	16; 100	1.76
PH_2**−Ir−PAu**[e]	$^1PH_2$	652	0.03	0.001	650	0.011	1.91
	^{3}PAu				706[g]	20; 150[g]	1.75[g]

[a] Acetonitrile at 298 K except for PH_2, dissolved in a mixture of acetonitrile/butyronitrile (2:1), butyronitrile at 77 K. [b] Energy levels from the emission maxima at 77 K. [c] Excitation at 355 nm, from ref 10. [d] Air equilibrated. [e] Excitation at 592 nm for steady state and at 532 nm for time resolved. [f] From ref 31. [g] Excitation at 405 nm for steady state and 532 nm for time-resolved experiments.

potentials observed are almost identical in the dyads and in the reference compounds. As a consequence, only weak interactions are expected between the components in the dyads and in the triads. Therefore localized description of the individual subunits could be used to predict exergonicity of energy and electron-transfer reactions. Due to the generally small shift observed between the redox potentials of arrays and the reference compounds it is difficult to conclude about ground-state donor−acceptor interactions. A more sensitive method such as electronic spectroscopy could permit a better detection (vide infra).

Photophysics

PH_2−Ir−PAu Triad and Related Models in Acetonitrile. Ground-State Absorption and Luminescence. The absorption spectrum of acetonitrile solutions of PH_2**−Ir−PAu** is reported in Figure 1 with those of the model components PH_2, **PAu**, and **Ir**. At 298 K, the luminescence intensity of the free base porphyrin is quenched in acetonitrile solutions of PH_2**−Ir** and of PH_2**−Ir−PAu** to about 99% and time-resolved emission experiments indicate that the lifetime of the singlet excited state of the free base is reduced from 8.3 ns to 30 ps in PH_2**−Ir** and PH_2**−Ir−PAu** (Table 2). The quenching does not occur in a butyronitrile glass at 77 K, where the lifetime of the model porphyrin, 11 ns, is maintained in both arrays (Table 2). The gold porphyrin does not emit at room temperature because of a very short singlet lifetime; at 77 K the phosphorescence of the triplet can be detected as a steady-state spectrum both in the model and in the arrays **PAu−Ir** and PH_2**−Ir−PAu**. Determination by time-resolved techniques (λ_{exc}= 532 nm) indicate that the phosphorescence of the gold porphyrin is present unquenched in both arrays at 77 K, displaying the typical biexponential decay of the gold porphyrin triplet of 10−20 μs and 100−150 μs. Table 2 summarizes the luminescence properties at 298 and 77 K for the arrays and the pertinent models together with the energy levels of the emitting states, derived from the emission maxima at 77 K.

Table 3. Transient Absorption Data for PH_2**−Ir−PAu** and Models at 298 K in Nitriles:[a] Excitation at 532 nm except Otherwise Specified

	state	τ (ns)	Φ[b]
PH_2	$^3PH_2$	200000	0.6[c]
PAu	^{3}PAu	1.4	1[c]
PH_2**−Ir**	$^3PH_2$	8000	0.1
	PH_2^+**−**Ir^-	0.075	1
PAu−Ir	^{3}PAu	1.4	1
PH_2**−Ir−PAu**	$^3PH_2$	2000	0.6
	^{3}PAu	1.4	1
	PH_2^+**−**Ir^-**−**PAu[d]	0.04	1
	PH_2^+**−Ir−**PAu$^-$[d]	3.5	0.5

[a] Acetonitrile except for PH_2, dissolved in a mixture of acetonitrile/butyronitrile (2:1). [b] Yields calculated on the basis of the photons absorbed by the PZn (or PAu) unit only. At 532 nm the partition of photons in the triad is: 25% on PH_2, 75% on PAu. In the dyads, the porphyrins absorb 100% light upon excitation in the visible. [c] From ref 31. [d] Selective excitation of PH_2 at 598 nm.

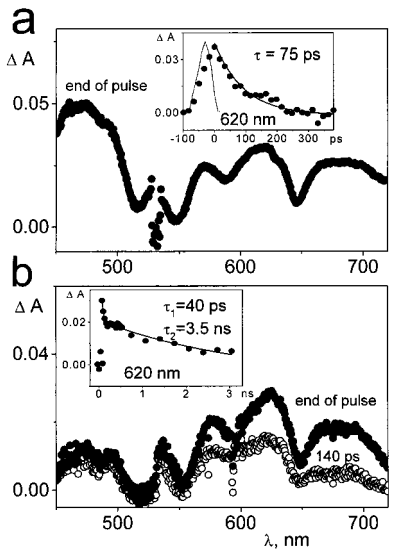

Figure 2. Transient absorbance changes upon selective excitation of the PH_2 unit by a 35 ps laser pulse. (a) Excitation at 532 nm (3 mJ) of acetonitrile solutions of PH_2**−Ir**, the inset shows the decay at 620 nm and the instrumental response (- - -). (b) Excitation at 598 nm (0.5 mJ) of acetonitrile solutions of PH_2**−Ir−PAu**, the inset shows the biexponential decay at 620 nm.

Time-Resolved Absorption. Transient absorbance determinations at ambient temperature (λ_{exc} = 532 nm) in acetonitrile solutions of PH_2**−Ir−PAu** and **PAu−Ir** allowed to detect the triplet state of the gold porphyrin which decays with a lifetime of 1.4 ns, typical of the model **PAu** in acetonitrile. An evaluation of the yield of formation of the gold porphyrin triplet, by taking into consideration only the photons absorbed by the gold porphyrin unit (calculated according to the ratio of the molar absorption coefficient of the components at 532 nm), gives a value identical to that of the model **PAu**, i.e., 1 (Table 3). Excitation at 532 nm of the dyad PH_2**−Ir** produces a selective excitation of the free-base porphyrin moiety. The resulting spectrum, Figure 2a, displays a maximum at 470 nm and a broad band in the region 600−700 nm with superimposed bleaching features of the Q-bands of the porphyrin at 645 nm. Its formation occurs during the laser pulse and is complete at the end of the

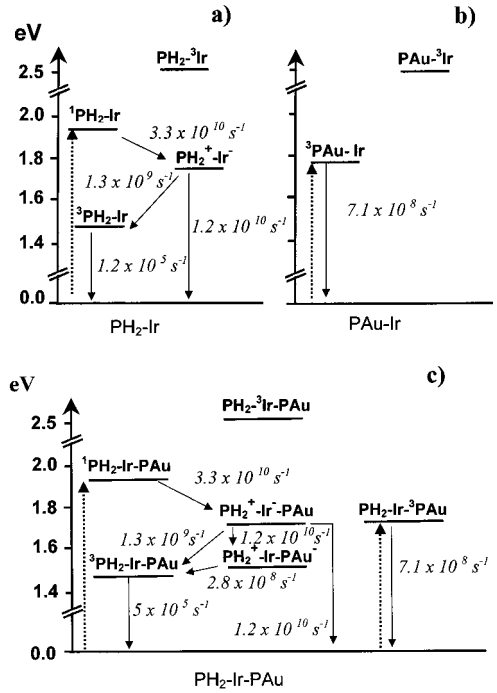

Figure 3. Schematic energy level diagram: (a) **PH_2−Ir**; (b) **PAu−Ir**; (c) **PH_2−Ir−PAu** in acetonitrile.

pulse; the decay is exponential with a lifetime of 75 ps and displays a complete recovery to the pre-pulse absorbance. Selective excitation of the PH_2 moiety was performed on the triad **PH_2−Ir−PAu** at 598 nm, by shifting with a Raman cell the 532 nm pulse (See Experimental Section for details). At the end of the pulse a spectrum very similar to the one detected for the dyad was recorded, which decayed faster than in the case of the dyad (40 ps lifetime) and evolved to a residual absorbance decaying with a lifetime of 3.5 ns (Figure 2b). Determinations performed by nanosecond laser flash photolysis over a wider time window give information on the triplet state localized on free-base porphyrin. The lifetime of this triplet in air-free acetonitrile is 8 μs for **PH_2−Ir** and 2 μs for **PH_2−Ir−PAu**, greatly reduced with respect to the model **PH_2** (200 μs). The absolute yield of these triplets in the dyad and triad were determined with respect to the photons absorbed by the free-base moiety only, and turned out to be 0.1 and 0.6 for **PH_2−Ir** and **PH_2−Ir−PAu** respectively. The results of transient absorbance experiments, both in the picosecond and in the nano- and microsecond range, are summarized in Table 3.

Photoinduced Processes. The above results can be interpreted on the basis of the current theories on photoinduced electron transfer.[19] As clearly shown by the spectroscopic and electrochemical data these arrays show a very modest electronic coupling between the components, and therefore can be discussed in terms of the properties of the individual components. A schematic energy level layout for the lowest states of the systems is reported in Figure 3. This has been drawn from the spectroscopic energy levels of the excited state (Table 2) and from a simplified evaluation of the energy of the charge-separated (CS) state which only takes into consideration the half wave potentials for the oxidation of the electron donor and the reduction of the electron acceptor in acetonitrile (Table 1).

(19) Marcus, R. A.; Sutin, N. *Biochim. Biophys. Acta* **1985**, *811*, 265 and references therein; Closs, G. L.; Miller, J. R. *Science* **1988**, *240*, 440 and references therein; *Electron Transfer-From Isolated molecules to biomolecules*, Part 1; Jortner J., Bixon, M., Eds.; John Wiley & Sons: New York, 1999.

The cases of the dyads will be discussed first. Upon excitation of **PH_2−Ir** in the visible, selective excitation to the singlet excited-state localized on the free-base porphyrin, **$^1PH_2$−Ir**, occurs. This state decays with a rate of 3.3×10^{10} s^{-1}, as determined in a time-resolved luminescence experiment, by a process which we assign to an electron-transfer reaction to form the CS state **PH_2^+−Ir^-**, where the transferred electron is localized on the terpy ligand of the complex. The absorption spectrum detected at the end of a 35 ps pulse and displayed in Figure 2a, consistent with the spectrum of a free-base porphyrin cation,[2,7] is assigned to this CS state. Its decay occurs with an overall rate of 1.33×10^{10} s^{-1}, in part to the underlying triplet state localized on the free base porphyrin, **$^3PH_2$−Ir**, and in part to the ground state. The yield of **$^3PH_2$−Ir**, 0.1, allows to derive the rate of the individual deactivation processes which are calculated to be 1.3×10^9 s^{-1} and 1.2×10^{10} s^{-1} for the deactivation to the triplet and to the ground state respectively (Figure 3a). In the case of the other dyad **PAu−Ir** (Figure 3b) the interpretation is straightforward: upon excitation in the visible only the gold porphyrin unit is excited and it behaves exactly as the model, irrespective of the appended iridium complex unit. This is expected since no energy transfer nor electron transfer (see Table 1 and Table 2), are feasible.

Inspection of Figure 3c, where the levels of the triad **PH_2−Ir−PAu** are reported, shows that in addition to the states already considered for the dyads, a further charge-separated state is present, corresponding to the oxidation of the PH_2 unit and the reduction of the PAu unit, **PH_2^+−Ir−PAu^-**. This state is lower in energy than the CS state already seen in the case of the dyad, with the hole localized on the free base and the electron localized on the terpy of the iridium complex, **PH_2^+−Ir^-−PAu,** and can be formed by the latter by a further electron-transfer step. Upon excitation at 532 nm both free-base porphyrin and gold porphyrin units are excited. The gold porphyrin triplet, **PH_2−Ir−^{3}PAu** which is detected by transient absorbance, behaves as the model and decays back to the ground-state irrespective of the presence of the other units. The free-base singlet, **$^1PH_2$−Ir−PAu**, can be detected by luminescence and displays a strong quenching (lifetime 30 ps) similar to the one detected in the case of the dyad **PH_2−Ir**. Therefore the quenching was assigned to the same electron-transfer process as in the model dyad, leading in this case to the CS state **PH_2^+−Ir^-−PAu**. Detection of this state by transient absorbance requires selective excitation at 598 nm of the free-base unit to prevent masking of the weak CS state absorbance by the gold porphyrin-localized triplet which displays a strong band around 620 nm. At the end of the 35 ps pulse at 598 nm, the spectrum is essentially identical to the one detected in the dyad (Figure 2a-b), therefore confirming our assignment to **PH_2^+−Ir^-−PAu**. The decay is nevertheless faster, the lifetime being 40 ps compared to 75 ps of the dyad, indicating that a further reaction competes to deplete this state with respect to the case of the dyad. The reaction is a further electron transfer step, leading to the fully CS state **PH_2^+−Ir−PAu^-** which is responsible for the residual absorbance after 140 ps (Figure 2b) and which decays with a lifetime of 3.5 ns. The reaction rate of this electron-transfer step can be calculated by comparison with the overall rate of decay of the dyad, 1.33 $\times$ 10^{10} s^{-1}, and turns out to be 1.2×10^{10} s^{-1}, from which a yield of formation of the fully CS state of 0.5 is derived. The recombination of the fully CS state can occur to the ground state but also to the triplet state localized on the free-base porphyrin **$^3PH_2$−Ir−PAu**, whose energy is ca. 0.1 eV lower. A determination of the yield of this triplet formation, 0.6, clearly indicates that the CS state quantitatively recombines to the triplet

localized on the free-base porphyrin. Formation of the excited triplet state of a component has often been reported in multicomponent synthetic arrays upon recombination of the charge separated state.[20,21] This is reminiscent of what is occurring in photosynthetic organisms in nature, where recombination of the primary charge-separated state to the triplet state of chlorophyll or bacteriochlophyll can take place in particular when the full charge separation event is precluded.[22] This process in the bacterial reaction center leads to sensitization of singlet oxygen and can kill the cell, in the absence of a suitable protection by carotenoids.[23]

In the dyad the CS state $\mathbf{PH_2}^+-\mathbf{Ir}^-$ decays rather fast and mainly to the singlet ground state while the fully CS state in the triad, $\mathbf{PH_2}^+-\mathbf{Ir}-\mathbf{PAu}^-$, recombines slower and essentially to the triplet state. The different behavior of the dyad and triad both in terms of lifetimes and in terms of spin multiplicity of the product of the recombination reaction are correlated and can be rationalized, having in mind that the primary CS state formed upon electron transfer from a singlet excited state has initially a singlet character and that recombination to a triplet state requires the change of the CS state to a triplet character. Recombination to the ground state has a rather high driving force, 1.55 eV for the triad and 1.75 eV for the dyad, which very likely places the reactions in the "Marcus inverted region" where the rate is expected to drop with increasing driving force. On the contrary, recombination to the triplet ($\Delta G = -0.08$ eV and $\Delta G = -0.28$ eV) are in the "normal" region.[19] In the case of $\mathbf{PH_2}^+-\mathbf{Ir}^-$ (and $\mathbf{PH_2}^+-\mathbf{Ir}^--\mathbf{PAu}$), the close coupling of the electron and hole, localized on the terpyridine ligand and on the π system of the tetrapyrrole macrocycle respectively, leads to a rapid charge recombination. By contrast, in $\mathbf{PH_2}^+-\mathbf{Ir}-\mathbf{PAu}^-$ the large distance between the hole and electron (ca. 2 nm) and the nature of the connecting bridge which is a poor conductor from the electronic viewpoint,[24] would make the recombination to the ground state slow. Therefore, while in the dyad there is little time for the original singlet to rephase, the longer lifetime of the fully CS state $\mathbf{PH_2}^+-\mathbf{Ir}-\mathbf{PAu}^-$ could allow for a spin rephasing of the original singlet CS state. Once the CS state has evolved to triplet, the recombination to the lower triplet state localized on the porphyrin $^3\mathbf{PH_2}-\mathbf{Ir}-\mathbf{PAu}$ can occur. A systematic study of the effect of the bridge length in an homogeneous series of donor−acceptor systems on the spin multiplicity of the charge recombination product has clearly shown that the ratio of triplet to singlet increases with the length of the bridge and also parallels the increase in lifetime of the CS state.[21] In the present case the presence of the heavy Ir(III) ion is expected to greatly favor the singlet-to-triplet conversion in the CS state by enhancing spin−orbit coupling. The same effect should be responsible for the increase of the intersystem crossing from the triplet localized on the free-base porphyrin to the ground-state singlet in the arrays, leading to a remarkable decrease of the triplet lifetime from 200 μs in the model PZn to 8 μs and 2 μs for $\mathbf{PH_2}-\mathbf{Ir}$ and $\mathbf{PH_2}-\mathbf{Ir}-\mathbf{PAu}$, respectively (Table 3). The absence of any porphyrin quenching at 77 K in a rigid glass is rationalized by the expected destabilization by several hundreds of meV of the CS state energy levels, caused by the rigidity of the solvent which does not allow reorientation about the CS state,[25] and would make endergonic the primary electron-transfer step.

After a thorough determination of the photophysical properties of the model units and model dyads it has been demonstrated that, upon excitation in the visible, the triad system $\mathbf{PH_2}-\mathbf{Ir}-\mathbf{PAu}$ can effectively yield charge separation with an efficiency of 0.5 and a resulting CS state with 3.5 ns lifetime. The presence of a low-lying triplet localized on the free-base porphyrin and the effect of the heavy Ir(III) ion in promoting a singlet-to-triplet spin rephasing offers the CS state an alternative deactivation through the triplet state.

PZn−Ir−PAu Triad and Related Models in Dichloromethane and Toluene. Stability and Solubility. As evidenced by the preparative procedures of the reference compounds and the various dyads and triads (heating at 140−196 °C), all the compounds studied are thermally very stable. The iridium(III)-containing component is photochemically extremely stable but the porphyrins can lead to photodecomposition, especially in nitrile solvent. Other solvents, namely dichloromethane and toluene, were used to overcome possible photochemical degradations. In toluene, the triad **PZn−Ir−PAu** and the reference compounds **PZn** and **PAu** are soluble whereas **PZn−Ir** and **PAu−Ir** are only very slightly soluble. All models and arrays, including the dyads **PZn−Ir** and **PAu−Ir** are soluble in dichloromethane. Surprisingly, in dichloromethane the model **PZn** displayed photochemical instability upon high energy laser irradiation but the arrays were perfectly stable and were studied in this solvent only. The reference iridium(III) complex **Ir** was insoluble both in toluene and dichloromethane but it could readily be dissolved in CH_3CN. For this compound, reference is made to properties displayed in acetonitrile solution.

Ground-State Absorption and Luminescence. The absorption spectra of **PZn**, **PAu** and **PZn−Ir−PAu** in dichoromethane is reported in Figure 4a with the spectrum of **Ir** in acetonitrile. Figure 4b shows the absorption of the same array and the model porphyrins in toluene, with the spectrum of **Ir** in acetonitrile. The luminescence of the PZn moiety in the arrays is nearly completely quenched in both solvents and time-resolved experiments indicate that the lifetime of the zinc porphyrin singlet is shorter than our resolution time, 20 ps (Table 4). The fluorescence of the zinc porphyrin moiety can be detected in the arrays in both solvents in glass at 77 K together with the phosphorescence bands localized on the triplet gold porphyrin and triplet zinc porphyrin. The luminescence data of the excited states at ambient temperature in the two solvents and the energy levels of the states, as derived from the emission maxima at 77 K, are summarized in Table 4.

Time-Resolved Absorption. Dichloromethane Solutions. Upon excitation of the PAu−Ir dyad at 532 nm with a 35 ps laser pulse, the triplet localized on the gold porphyrin is formed, with the typical band around 620 nm and a lifetime of 1.4 ns, as displayed by the model PAu in the same solvent (Table 5). Selective excitation of the PZn unit in PZn−Ir yields a transient spectrum with an intense band maximized at 670 nm, decaying

(20) Hasharoni, K.; Levanon, H.; Greenfield, S. R.; Gosztola, D. J.; Svec, W. A.; Wasielewski, M. R. *J. Am. Chem. Soc.* **1995**, *117*, 8055. Maggini, M.; Guldi, D. M.; Mondini, S.; Scorrano, G.; Paolucci, F.; Ceroni, P.; Roffia, S. *Chem. Eur. J.* **1998**, *4*, 1992. Kuciauskas, D.; Liddell, P. A.; Moore, A. L.; Moore, T. A.; Gust, D. *J. Am. Chem. Soc.* **1998**, *120*, 10880. Martin, N.; Sánchez, L.; Herranz, M. A.; Guldi, D. M.. *J. Phys. Chem.* A **2000**, *104*, 4648.

(21) Roest, M. R.; Oliver, A. M.; Paddon-Row, M. N.; Verhoeven, J. W. *J. Phys. Chem.* A **1997**, *101*, 4867.

(22) See for example: Regev, A.; Nechustai, R.; Levanon, H.; Thornber, J. P. *J. Phys. Chem.* **1989**, *93*, 2421.

(23) Griffith, M.; Sistrom, W. R.; Cohen-Bazire G.; Stanter, R. Y. *Nature* **1955**, *176*, 1211. Cogdell, R. J.; Frank, H. A. *Biochim. Biophys. Acta* **1987**, *895*, 63.

(24) A similar Ru(II) bis-terpy bridge was shown to be a modest electron conductor in a triplet−triplet energy transfer process occurring in a similar porphyrinic array by a Dexter mechanism and involving electron and hole migration through the bridging complex.[8b]

(25) Gaines, G. L., III; O'Neil, M. P.; Swec, W. A.; Niemczyk, M. P.; Wasielewski, M. R.*J. Am. Chem. Soc.* **1991**, *113*, 719.

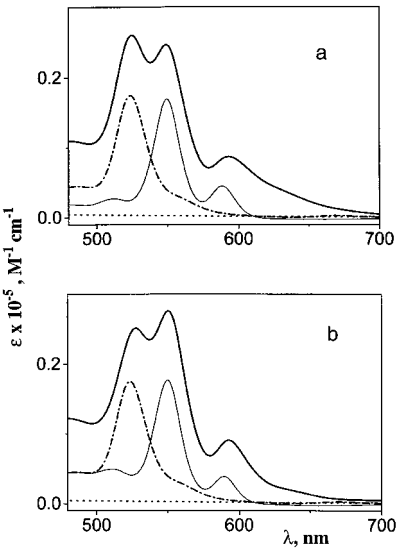

Figure 4. Molar absorption coefficients of the models **PZn** (—), **PAu** (-·-·-) and of the triad **PZn**−**Ir**−**PAu** (—) in dichloromethane solutions. **Ir** (···) is in acetonitrile solution.

Table 4. Luminescence Properties and Energy Levels of the Excited States of **PZn**−**Ir**−**PAu** and Models in Dichloromethane[a] and Toluene;[b] **Ir** Is Insoluble in Both Solvents, Dyads **PZn**−**Ir** and **PAu**−**Ir** Are Insoluble in Toluene

		298 K			77 K	
	state	$\lambda_{max\ (nm)}$	τ (ns)	Φ_{fluo}	$\lambda_{max\ (nm)}$	E (eV)[b]
PZn[a]	^{1}PZn[c]	596	1.8	0.064	606	2.05
	^{3}PZn[c]				770	1.61
PZn[b]	^{1}PZn[c]	596	2.2	0.08	596	2.08
	^{3}PZn[c]				776	1.60
PAu[a]	^{3}PAu[d]				712	1.74
PAu[b]	^{3}PAu[d]				712	1.74
PZn−**Ir**[a]	^{1}PZn[c]		≤ 0.020	1×10^{-4}	620	2.00
	^{3}PZn[c]				790	1.57
PAu−**Ir**[a]	^{3}PAu[d]				712	1.74
PZn−**Ir**−**PAu**[a]	^{1}PZn[c]		≤ 0.020	8×10^{-5}	614	2.02
	^{3}PZn[c]				790	1.60
	^{3}PAu[d]				716	1.73
PZn−**Ir**−**PAu**[b]	^{1}PZn[c]		≤ 0.020	6×10^{-4}	606	2.05
	^{3}PZn[c]				786	1.58
	^{3}PAu[d]				716	1.73

[a] Dichloromethane. [b] Toluene. [c] Excitation at 560 nm for steady state; correction for the absorbance of other units in the array was applied when necessary. Excitation at 532 nm for time resolved. [d] Excitation at 405 nm.

with a lifetime of 120 ps (Figure 5a). The spectrum is consistent with that of a Zn porphyrin cation[2,7] and assigned to the PZn$^+$−Ir$^-$ charge-separated state. Upon excitation of the triad PZn−Ir−PAu at 532 nm, both the PZn unit and the PAu units absorb photons, 25% and 75% respectively, as derived by the molar absorption coefficients of the components. The results of picosecond transient absorption experiments are reported in Figure 5b. The spectrum at the end of the pulse, displaying a maximum around 640 nm, decays with a lifetime of 110 ps in a spectral region maximized around 670 nm, where the species detected in the dyad shows a strong band. Therefore this band is assigned to the same transient as in the dyad, the CS state **PZn**$^+$−**Ir**$^-$−**PAu**. The absorption recorded 170 ps after the end of the pulse is typical of the triplet localized on the gold porphyrin, with a band at 620 nm and a lifetime of 1.4 ns. Experiments on a longer time scale by a nanosecond laser photolysis apparatus showed that in air-free dichloromethane solutions no residual absorbance was left after the decay of the above species, and no triplet localized on the zinc porphyrin could be detected. This indicates an upper limit of 0.05 for the yield of the ^{3}PZn−Ir−PAu state (Table 5).

Table 5. Transient Absorption Data for **PZn**−**Ir**−**PAu** and Models in Dichloromethane[a] and Toluene, [b]Excitation at 532 nm; **Ir** Is Insoluble in Both Solvents, Dyads **PZn**−**Ir** and **PAu**−**Ir** Are Insoluble in Toluene

	state	τ (ns)	Φ[c]
PZn[a]	^{3}PZn	250000	1
PZn[b]	^{3}PZn	300000	1
PAu[a]	^{3}PAu	1.4	1
PAu[b]	^{3}PAu	2.5	1
PZn−**Ir**[a]	^{3}PZn		< 0.05
	PZn$^+$−Ir$^-$	0.120	
PAu−**Ir**[a]	^{3}PAu	1.4	1
PZn−**Ir**−**PAu**[a]	^{3}PZn		< 0.05
	^{3}PAu	1.4	1
	PZn$^+$−Ir$^-$−PAu	0.110	
	PZn$^+$−Ir−PAu$^-$		
PZn−**Ir**−**PAu**[b]	^{3}PZn	7000	≤ 0.1
	^{3}PAu	2.5	
	PZn$^+$−Ir$^-$−PAu	≤ 0.020	
	PZn$^+$−Ir−PAu$^-$	450	*d*

[a] Dichloromethane. [b] Toluene. [c] Relative yields calculated on the basis of the photons absorbed by the PZn (or PAu) unit only. At 532 nm the partition of photons in the triad is in dichloromethane: 25% on PZn, 75% on PAu, in toluene: 28% on PZn, 72% on PAu. In the dyads only the porphyrins absorb light upon visible excitation. [d] The absolute yield is measured to be 1.2 ± 0.3 (See text)

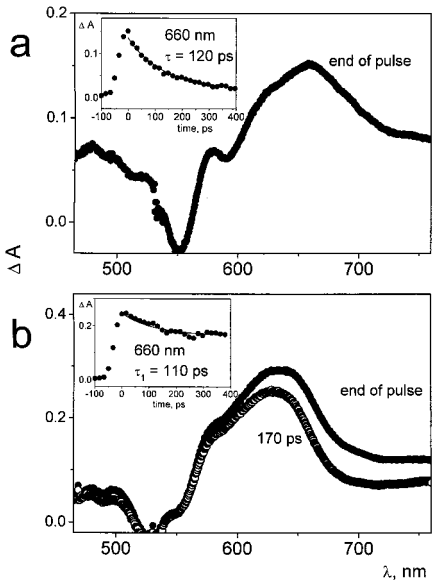

Figure 5. Transient absorbance changes upon excitation at 532 nm (35 ps pulse, 3.5 mJ) in dichloromethane solutions. (a) **PZn**−**Ir**, spectrum at the end of the laser pulse; the inset shows the decay at 660 nm. (b) **PZn**−**Ir**−**PAu**, spectrum at the end of the pulse (●) and at 170 ps after the end of pulse (O); the inset shows the decay at 660 nm.

Toluene Solutions. The properties of the models are reported in Table 5; to note that the lifetime of the gold porphyrin triplet is increased to 2.5 nanoseconds in this solvent with respect to the 1.4 ns of acetonitrile and dichloromethane solutions. Upon excitation of **PZn**−**Ir**−**PAu** at 532 nm both PZn and PAu units absorb photons, 28% and 72% respectively. The spectrum detected at the end of a 35 ps pulse at 532 nm (Figure 6) shows a red-shifted absorption with a stronger band below 500 nm with respect to the spectrum of **^{3}PAu** (reported in the same figure). Therefore in **PZn**−**Ir**−**PAu** there is, in addition to the absorbance of the **^{3}PAu**, a contribution from a species with a band maximized around 670 nm which is formed faster than

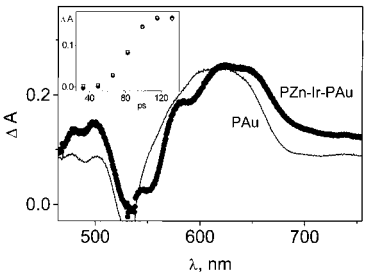

Figure 6. Transient absorbance changes upon excitation at 532 nm (35 ps pulse, 3.5 mJ) detected at the end of the pulse in a toluene solution of **PZn−Ir−PAu** (●) and **PAu** (—). The inset shows the rise at 680 nm of the transient absorbance in **PZn−Ir−PAu** (●) compared to the rise of a standard (▽) whose formation is immediate with the laser excitation (See Experimental Section for details).

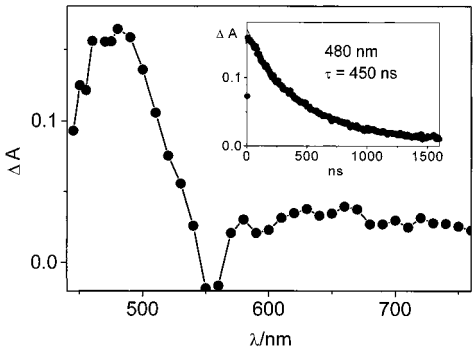

Figure 7. Transient absorbance changes upon excitation at 532 nm (18 ns pulse, 1 mJ) detected at the end of the pulse in a toluene solution of **PZn−Ir−PAu.** In the inset the decay of the spectrum in air-free toluene solution is reported.

our resolution, since its rise time cannot be resolved from the instrumental response (inset of Figure 6). After the decay of the gold porphyrin triplet, which occurs with a lifetime of ca. 2.5 ns as in the model, the former absorbance maximized around 670 nm is left as a residual. It can be detected unaltered in a nanosecond laser flash photolysis experiment, where the spectrum reported in Figure 7 is registered at the end of a 18 ns laser pulse at 532 nm. The lifetime of this species in air-free solution is 450 ns (inset of Figure 7) and is unaffected by the concentration of the array in the solution and by the energy of the laser; air equilibration reduces the lifetime to 310 ns. On the basis of spectral and kinetic evidences such species is identified as the CS state $\mathbf{PZn^{+}-Ir-PAu^{-}}$. In air-free solution a rather weak transient absorbance is left after the decay of the 450 ns species; this has a lifetime of 7 μs and a spectrum consistent with that of the triplet zinc porphyrin. The yield of formation of the zinc porphyrin triplet $\mathbf{^3PZn-Ir-PAu}$ calculated against $\mathbf{^3PZn}$ and taking into consideration the photons absorbed by the PZn unit only is ≤ 0.1. The data derived by transient absorbance determinations are summarized in Table 5.

Photoinduced Processes. The results obtained with the system **PH₂−Ir−PAu**, previously discussed, show that a deactivation path to a low-lying triplet is rate determining for the lifetime of the CS state $\mathbf{PH_2^{+}-Ir-PAu^{-}}$. The study on the zinc porphyrin derivative was undertaken because, given the higher energy of the excited states (Tables 2 and 4) and the stronger reductant ability of the PZn unit with respect to the PH_2 unit (Table 1), an inversion in the energy ordering of the CS state and the triplet state was expected.

Dichloromethane Solutions. The schematic energy levels for the dyads **PZn−Ir**, **PAu−Ir** and the triad **PZn−Ir−PAu**

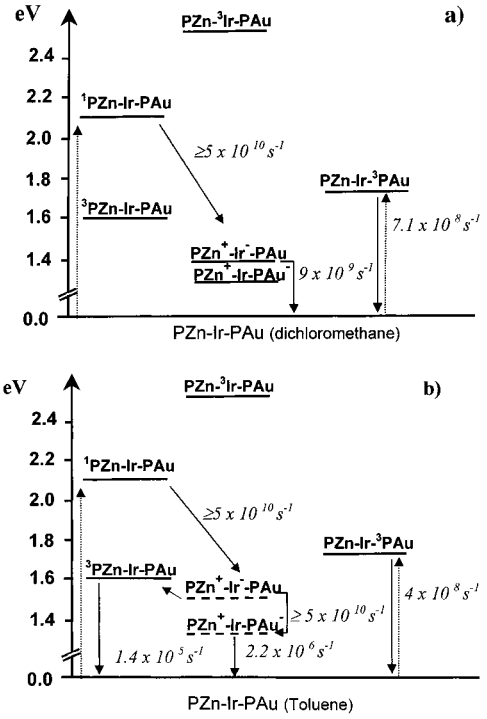

Figure 8. Schematic energy level diagram: (a) **PZn−Ir−PAu** in dichloromethane (b) **PZn−Ir−PAu** in toluene. The CS state levels are based on electrochemical data in dichloromethane, with some adjustment for solvent polarity considerations (see text).

in dichloromethane confirm the above expectations (Figure 8a). The absence of alternative possibility of deactivation for $\mathbf{PZn^{+}-Ir-PAu^{-}}$ is expected to greatly enhance the lifetime of the CS state which now can only deactivate directly to the ground state, a process characterized by a large driving force (ΔG ca. −1.35 eV) very likely falling in the "Marcus inverted region".[19] Unfortunately, the fully CS state in CH_2Cl_2 could never be detected as explained below.

The absorption spectra in dichloromethane solutions (Figure 4a) indicate that in this solvent the spectrum of the array is not the simple superimposition of the components but there is a broad tail extending from 600 to 700 nm. This could be ascribed to the presence of a charge-transfer band due to the interaction in the ground state between the reductant PZn ($E_{1/2} = 0.68$ V vs SCE) and the oxidant Ir ($E_{1/2} = -0.71$ V vs SCE). The tail is not present, or present to a much lower extent in the apolar toluene solvent (Figure 4b) which supports our assignment. The existence of charge-transfer interactions in the ground state between the components in multicomponent porphyrinic systems containing a good electron acceptor has been reported before.[26]

Excitation of **PZn−Ir** in the visible range produces the singlet excited-state localized on the zinc porphyrin unit, $\mathbf{^1PZn-Ir}$, which decays with a rate $\geq 5 \times 10^{10}$ s^{-1}, faster than our resolution in the luminescence experiments (20 ps). The absorption spectrum of the product (Figure 5a) displays a maximum at 660−670 nm typical of the zinc porphyrin cation, arising from the CS state $\mathbf{PZn^{+}-Ir^{-}}$, which decays by charge recombination with a rate of 8.3×10^9 s^{-1}. The dyad **PAu−Ir** does not show any difference in reactivity with respect to that of the chromophore **PAu**. The behavior of the triad **PZn−Ir−PAu** in dichloromethane (Figure 8a) is rather different from that of the related **PH₂−Ir−PAu** in acetonitrile (Figure 3c).

(26) Armaroli, N.; Marconi, G.; Echegoyen, L.; Bourgeois, J.-P.; Diederich, F. *Chem. Eur.J.* **2000**, *6*, 1629

Once the primary electron transfer has occurred to yield **PZn**$^+$−**Ir**$^-$−**PAu**, with a rate ≥ 5×10^{10} s^{-1} as in the case of the model dyad, the electron-transfer reaction does not proceed further to form **PZn**$^+$−**Ir** −**PAu**$^-$, but **PZn**$^+$−**Ir**$^-$−**PAu** decays back to the ground state with approximately the same rate displayed by the dyad, 9×10^9 s^{-1}.

The reason for the inefficiency of the secondary forward electron transfer in the **PZn**−**Ir**−**PAu** triad, can be explained by the simultaneous occurrence of unfavorable thermodynamic and electronic parameters. The driving force for the secondary electron-transfer step is in fact very small ($\Delta G = -0.05$ eV) and this would be sufficient to make the reaction inefficient. In addition, the presence of a charge transfer interaction in the ground state between the PZn and Ir units, as suggested by the ground state absorption spectrum, could result in the presence of a corresponding low energy excited state with a charge transfer character (exciplex). This state, localized on the PZn and the Ir units, could be strongly mixed with the true CS state **PZn**$^+$−**Ir**$^-$−**PAu**. As a consequence of the mixing the distribution of the extra electron on the ligands of the Ir unit in the CS state **PZn**$^+$−**Ir**$^-$−**PAu** could be rather unsymmetrical, with a higher probability for the electron to be localized on the terpy close to the PZn. This circumstance would make more difficult the subsequent electron-transfer step to the gold porphyrin unit, linked on the opposite terpy. Direct detection of an exciplex state and its role in the formation of charge-separated states in a similar donor−acceptor array has been recently reported.[27]

Toluene Solutions. The energy level diagram in toluene is reported in Figure 8b. The energy levels are essentially similar to those in dichloromethane, except for the CS state levels which we expect to be affected by the different polarity of the two solvents.

No electrochemical data are available in this solvent and we can only make qualitative considerations on the basis of the different polarities of the two media. **PZn**−**Ir** is insoluble in this solvent and a good piece of information is missing. In any case our experimental observations on **PZn**−**Ir**−**PAu** tell us that, upon quenching of the luminescence of zinc porphyrin with a rate ≥ 5×10^{10} s^{-1}, a spectrum appears within our resolution (20 ps) and contains a contribution, in addition to that of **PZn**−**Ir**−^{3}**PAu**, of a long-lived species with a strong band around 660−670 nm. The lifetime of the species is 450 ns in air-free solution, rather different from that of the triplet ^{3}**PZn** which is 7 μs in this experiment. The spectral features are in full agreement with those of the zinc porphyrin cation and we identify this species as the fully CS state **PZn**$^+$−**Ir**−**PAu**$^-$, formed by a very fast (k ≥ 5×10^{10} s^{-1}) secondary electron transfer from **PZn**$^+$−**Ir**$^-$−**PAu**. An estimation of the yield of the fully CS state measured against the photons absorbed by the PZn moiety can come from the literature spectroscopic data of the zinc tetraphenylporphyrin cation[28] and this results in 1.2 ± 0.3 (See Experimental Section for details).

Comparison of PZn−Ir−PAu Behavior in Dichloromethane and in Toluene Solutions. The reason for the different behavior of the triad in toluene with respect to dichloromethane has mainly to be assigned to the absence in the former of a charge transfer interaction between the PZn and Ir units, as shown from the ground state absorption spectra, but also very likely to a higher driving force for the **PZn**$^+$−**Ir**$^-$−**PAu** → **PZn**$^+$−**Ir**−**PAu**$^-$ electron-transfer reaction in toluene. In fact, in the less polar toluene both CS states and the ground state are destabilized with respect to the more polar dichloromethane but **PZn**$^+$−**Ir**$^-$−**PAu** is expected to be more destabilized than **PZn**$^+$−**Ir**−**PAu**$^-$ with respect to the ground state **PZn**−**Ir**−**PAu**. This can be explained, in a rather qualitative approach, with the distribution of charges on the units of the array in the ground and CS states. In **PZn**$^+$−**Ir**−**PAu**$^-$ the charge distribution is: +1, +3, 0, i.e., identical, but reverse with respect to the ground state **PZn**−**Ir**−**PAu**: 0, +3, +1. Therefore we expect that the energy gap between the final CS state **PZn**$^+$−**Ir**−**PAu**$^-$ and the ground state is little affected by the polarity of the solvent. In **PZn**$^+$−**Ir**$^-$−**PAu**, on the contrary, the charge distribution is +1, +2, +1 and a less polar solvent (toluene) could stabilize less this state with respect to the ground state than a more polar solvent (dichloromethane) can. In conclusion we expect that the energy level of **PZn**$^+$−**Ir**$^-$−**PAu** is raised in energy when in toluene solutions while the **PZn**$^+$−**Ir**−**PAu**$^-$ state remains nearly unaltered with respect to the energy level in dichloromethane solutions. This would affect slightly the driving force for the primary electron transfer (0.66 eV in dichloromethane) which still remains very fast, but would increase the driving force for the secondary electron transfer (0.05 eV in dichloromethane), allowing for the secondary electron transfer to compete efficiently with the back recombination in the case of toluene. The increase in the level of **PZn**$^+$−**Ir**$^-$−**PAu** in toluene with respect to dichloromethane could also explain the formation of a sizable amount of triplet ^{3}**PZn**−**Ir**−**PAu**, whose energy level is now nearly iso-energetic with the primary CS state **PZn**$^+$−**Ir**$^-$−**PAu** (Figure 8b and Table 5).

Conclusion

Two triads incorporating iridium (III) as assembling metal and playing the role of electron relay and two different porphyrins respectively electron donor (PH_2 or PZn) and secondary electron acceptor (PAu) have been synthesized and characterized. Their electrochemical and photophysical properties have been studied in the light of the properties of corresponding dyads (**PH_2**−**Ir**, **PZn**−**Ir**, **PAu**−**Ir)** and individual components (**PH_2**, **PZn**, **PAu)**.

The photoinduced processes observed in the dyads and triads are very dependent on thermodynamic parameters as well as on the nature of the solvent. It has been demonstrated that in acetonitrile the triad **PH_2**−**Ir**−**PAu** leads to a fully CS state with a lifetime of 3.5 ns. The energy ordering of the triplet state of **PH_2** and of the final CS state **PH_2**$^+$−**Ir**−**PAu**$^-$ is responsible of this short lifetime. For the triad **PZn**−**Ir**−**PAu** in dichoromethane the primary electron-transfer to yield **PZn**$^+$−**Ir**$^-$−**PAu** is not followed by a secondary electron transfer due to both thermodynamic and electronic unfavorable parameters. By contrast, in toluene, **PZn**−**Ir**−**PAu** has been shown to yield, upon excitation in the visible region, a fully charge-separated state with a unitary yield and a lifetime of 450 ns. It is interesting to note that the two electron-transfer processes leading to the CS state are very fast and could not be time-resolved. Contrary to the most common expectations, full charge separation occurs in an apolar solvent and not in a more polar solvent, where charge-transfer interactions in the ground state and a too small driving force preclude the efficient completion of the sequential electron-transfer steps. In an apolar solvent, ground state-charge-transfer interactions are suppressed and a different stabilization of the intermediate and final CS states determines the favorable conditions for an efficient and complete sequential electron transfer.

(27) Tkachenko, N. V.; Rantala, L.; Tauber, A. Y.; Helaja, J.; Hynninen, P. H.; Lemmetyinen, H. *J. Am. Chem. Soc*. **1999**, *121*, 9378.
(28) Fajer, J.; Borg, D. C.; Forman, A.; Dolphin, D.; Felton, R. H. *J. Am. Chem. Soc*. **1970**, *92*, 3451.

Experimental Section

Photophysics. The solvents used for photophysical determinations are Spectroscopic Grade (C. Erba). Absorption spectra were recorded with a Perkin-Elmer Lambda 9 spectrophotometer. Uncorrected emission spectra were detected by a Spex Fluorolog II spectrofluorimeter, which was equipped with a phosphorimeter accessory (1934D) for the determination of phosphorescence spectra. Time-resolved luminescence apparatus was based on a Nd:YAG laser (35 ps pulse duration, 532 nm, 1 mJ) and a Streak Camera.[29] Lifetimes longer than 2 ns were detected with a Time Correlated Single Photon Counting apparatus with 1 ns resolution Phosphorescence lifetimes were determined by a Nd:YAG laser (18 ns pulse, 532 nm, 2 mJ) and a photomultiplier Hamamatsu R936.[30]

Transient absorbance in the picosecond range made use of a pump and probe system based on a Nd:YAG laser (35 ps pulse, 532 nm, 2−4 mJ) and an OMA detector.[31] The instrumental response profile was obtained by measuring the buildup of the absorption of a solution of DODCI (3−3′-diethyloxadicarbocyanine) in methanol at 450 nm.[32] Zero time was assumed to be at the complete evolution of the absorption of the sample. For excitation at 598 nm the second harmonic (532 nm) was Raman shifted by a C_6D_{12} cell: 30 mJ at 532 were collimated on a 10 cm cell, the resulting Raman line at 598 nm was selected by colored filters and the residual 532 nm wave was diverted by a dichroic 45 degree mirror. The energy at 598 nm was ca. 0.5 mJ.

Yields and lifetime of absorbing species in the 10 ns-1000 μs range were determined by a laser flash photolysis apparatus with a Nd:YAG laser (18 ns pulse, 532 nm, 2−4 mJ).[33] The yields of triplets in the arrays were determined against the model porphyrin in the same solvent as a standard, by comparing absorbances of the triplets at wavelength longer than ground-state absorbance (620 nm for **PAu**, 650 nm for **PZn**, 680 nm for **PH_2**). The yield of the state **PZn^+−Ir−PAu^-** was determined by using a molar absorption coefficient of 1×10^4 $M^{-1}cm^{-1}$ at 680 nm[28] and as actinometer was used zinc tetraphenylporphyrin in toluene with a triplet yield of 0.81 and a $\Delta\epsilon$ at 470 nm of 7.3×10^4 M^{-1} cm^{-1}.[34]

Air-free solutions were bubbled with argon for 5 min and stored in a vacuum tight homemade cells. For luminescence experiments at 77 K, quartz capillary tubes were immersed in liquid nitrogen contained in a homemade quartz dewar.

Electrochemistry. Cyclic voltammetry was carried out in MeCN or CH_2Cl_2 solution, using Bu_4NPF_6 as supporting electrolyte, a Pt working electrode, a Pt counter-electrode, and SCE as reference. The typical sweep rate was 100 mV/s, and the window used was from −1.4V to +1.3V. Some waves were poorly reversible, probably due to the adsorption of the species on the electrode.

Synthesis. The commercial starting materials were obtained from Acros, Aldrich, Fluka, Lancaster, or Merck. $IrCl_3 \cdot 4H_2O$ was obtained from Pressure Chemical Co., and $IrCl_3$ was given by Johnson Matthey. Some starting materials were prepared following literature procedures: 4′-formylphenyl-2,2′:6′,2″-terpyridine,[35] 4′-bromo-2,2′:6′,2″-terpyridine,[13] 4′(3,5-ditertiobutylphenyl)-2,2′:6′,2″-terpyridine (Ar-terpy),[10] and Ir(Ar-terpy)Cl_3.[10] The solvents were distilled over the appropriate drying agents, and pyrrole was filtered over alumina before use. All charged species were isolated as PF_6 salts. In the NMR assignments, the protons of the terpyridines are referred to as Ar-tpy, PH_2-tpy, or PAu-tpy, the protons of the para-phenylene spacers are labeled 1 and 2. The protons on the 3,5-di^{t}BuPh groups are labeled o,o′ and p,p′ on a porphyrin and o″ and p″ on Ar-tpy.

8. 4-Formylphenylboronic acid (1 g, 6.67 mmol) and 2,2-dimethylpropane-1,3-diol (695 mg, 6.67 mmol) were refluxed in distilled benzene (20 mL) for 2h30. The crude mixture was evaporated to dryness, and ^{1}H NMR showed the reaction to be quantitative (1.45 g of colorless solid). ^{1}H NMR (200 MHz, $CDCl_3$), (ppm): 10.05 (s, 1H, CHO); 7.97 (d, 2H, H_{Ar}, $^3J = 8.1$ Hz); 7.85 (d, 2H, H_{Ar}, $^3J = 8.1$ Hz); 3.80 (s, 4H, CH_2); 1.05 (s, 6H, CH_3).

9. All the glassware was dried in an oven and allowed to cool in a desiccator. Compound **8** (400 mg, 1.84 mmol) and 3,5-ditertiobutylbenzaldehyde (1.2 g, 5.52 mmol, 3 eq) were placed in a 1-L three-necked flask. Chloroform (750 mL) was transferred into the reaction flask via cannula. This mixture was degassed and stirred for 10 min under argon. Pyrrole (0.51 mL, 7.5 mmol, 4 eq) was injected with a syringe. This mixture was stirred for 10 min. Boron trifluoride etherate (0.28 mL, 2.2 mmol, 1.2 eq) was added with a syringe, the solution immediately turning yellow. This mixture was stirred in the dark for 1h30, during which the solution darkened. Chloranil (1.97 g, 8 mmol, excess) was added, the argon inlet was replaced by a silicagel tube and the mixture was refluxed for 30 min. After cooling to room temperature (RT), the crude reaction mixture was washed with water (2 × 250 mL) and evaporated to dryness. It was purified by repeated chromatography on silica, eluted with CH_2Cl_2 (up to 3% MeOH) and gave 80 mg of the desired unsymmetrical porphyrin **9** (4%), and 10 mg of symmetrical (trans) bis-boronic porphyrin (0.5%). Other fractions (150 mg overall) contained a mixture of pure **9** and bis-boronic porphyrin. ^{1}H NMR (A_3B, **9**) (200 MHz, $CDCl_3$), δ (ppm): 8.92−8.85 (m, 8H, pyrroles); 8.26 (d, 2H, H_1, $^3J = 7.7$ Hz); 8.19 (d, 2H, H_2, $^3J = 7.7$ Hz); 8.10 (s, 6H, H_o); 7.81 (s, 3H, H_p); 3.96 (s, 4H, CH_2); 1.54 (s, 54H, ^{t}Bu); 1.19 (s, 6H, CH_3); −2.65 (broad s, 2H, NH). ^{1}H NMR (trans-A_2B_2, bis-boronic porphyrin) (200 MHz, $CDCl_3$), δ (ppm): 8.88 (d, 4H, pyrroles, $^3J = 4.7$ Hz); 8.84 (d, 4H, pyrroles, $^3J = 4.7$ Hz); 8.24 (d, 2H, H_1, $^3J = 8$ Hz); 8.18 (d, 2H, H_2, $^3J = 8$ Hz); 8.09 (d, 4H, H_o, $^4J = 1.7$ Hz); 7.80 (t, 2H, H_p, $^4J = 1.7$ Hz); 3.95 (s, 8H, CH_2); 1.55 (s, 36H, ^{t}Bu); 1.18 (s, 12H, CH_3); −2.72 (s, 2H, NH).

1. All solutions were carefully degassed before their introduction in the reaction flask. 4′-Bromoterpy (31 mg, 0.098 mmol) was placed in a 50-mL two-necked flask. Toluene (1 mL) was added, followed by solid $Pd(PPh_3)_4$ (23 mg, 0.2 eq) and a 2M aqueous solution of sodium carbonate (0.5 mL). A solution of **9** (104 mg, 0.098 mmol) was transferred via cannula, first by partially dissolving the porphyrin in absolute EtOH (2.5 mL) and subsequently dissolving the rest with toluene (3 × 2 mL). After degassing once more, the reaction mixture was heated at 100 °C and under argon for 24 h. The crude mixture was chromatographed on Al_2O_3 (from pure hexane to pure CH_2Cl_2) to yield 92 mg of **1** (0.077 mmol, 79%). ^{1}H NMR (200 MHz, $CDCl_3$), δ (ppm): 9.09 (s, 2H, $H_{3'}+H_{5'}$), 8.94 (m, 8H, pyrroles), 8.83 (m, 2H, H_3), 8.80 (m, 2H, H_6), 8.42 (d, 2H, H_2, $^3J = 8.4$ Hz), 8.32 (d, 2H, H_1, $^3J = 8.4$ Hz), 8.13 (d, 4H, H_o, $^4J = 2$ Hz), 8.11 (d, 2H, $H_{o'}$, $^4J = 2$ Hz), 7.96 (ddd, 2H, H_4, $^3J = 7.7$ Hz, $^4J = 2$ Hz), 7.82 (m, 3H, $H_p+H_{p'}$), 7.42 (ddd, 2H, H_5, $^3J = 7.7$ Hz, $^4J = 1.4$ Hz), 1.55 (s, 54H, ^{t}Bu), −2.64 (s, 2H, NH). MS (FAB^+), *m/z*: 1182.9 ($[M]^+$).

2^+ (PAu). Compound **1** (55 mg, 0.047 mmol), $KAuCl_4$ (44 mg, 0.117 mmol), and NaOAc (15.2 mg, 0.185 mmol) were heated to reflux in degassed AcOH (5 mL), under argon and in the dark, for 8 h. UV−Visible absorption spectroscopy confirmed the disappearance of about 90% of the free-base porphyrin. AcOH was evaporated and the crude mixture was dissolved in CH_2Cl_2 and washed with a 0.2M aqueous KPF_6 solution. The organic layer was washed with 5% aqueous Na_2CO_3 (4 × 100 mL) and with water (3 × 100 mL). The aqueous layer was extracted with CH_2Cl_2 (3 × 50 mL), dried over $MgSO_4$ and filtered. $MgSO_4$ was stirred with CH_2Cl_2 overnight. The organic layers were combined, evaporated and chromatographed on alumina (CH_2Cl_2/EtOH, 0−15%) to give 2^+ as a deep red-orange solid in 89% yield (63 mg).

3^{4+} (PAu−Ir). 2^+ (15 mg, 0.098 mmol) and Ir(Ar-tpy)Cl_3 (7 mg, 0.097 mmol) were heated to 140 °C in degassed ethylene glycol (5 mL), under argon and in the dark, for 3 h. The solvent was evaporated under reduced pressure. The crude mixture was dissolved in acetone, precipitated by the addition of a 0.2M aqueous KPF_6 solution and filtered. After chromatography on silica (acetone/water/saturated aqueous KNO_3 solution: 100/0/0 to 95/10/0.2), anion exchange with KPF_6, chromatography on fine silica (same eluent: 100/0/0 to 100/10/0.5)

(29) Flamigni, L. *J. Phys. Chem.* **1993**, *97*, 9566.
(30) Flamigni, L.; Armaroli, N.; Barigelletti, F.; Chambron, J.-C.; Sauvage, J.-P., Solladié, N.*New J. Chem.* **1999**, *23*, 1151.
(31) Flamigni, L.; Armaroli, N.; Barigelletti, F.; Balzani, V.; Collin, J.-P.; Dalbavie, J.-O.; Heitz, V.; Sauvage, J.-P. *J. Phys. Chem.* **1997**, *101*, 5936.
(32) Flamigni, L. *J. Phys. Chem.* **1992**, *96*, 3331.
(33) Hubig, S. M.; Rodgers, M. A. J. In *Handbook of Organic Photochemistry*; Scaiano, J. C., Ed.; C.R.C. Press: Boca Raton, FL, 1989; Vol. I, Chapter 13.
(34) Tanelian, C.; Wolff, C. *J. Phys. Chem.* **1995**, *99*, 9825.
(35) Collin, J.-P.; Heitz, V.; Sauvage, J.-P. *Tetrahedron Lett.* **1991**, *32*, 5977.

and anion exchange again, $\mathbf{3}^{4+}$ was obtained in a 96% yield (24 mg, 0.093 mmol) as a red solid. ^{1}H NMR (400 MHz, $CDCl_3$), δ (ppm): 9.50 (d, 2H, pyrroles, ^3J = 5.2 Hz); 9.42 (d, 2H, pyrroles, ^3J = 5.2 Hz); 9.41 (d, 2H, pyrroles, ^3J = 5.4 Hz); 9.37 (d, 2H, pyrroles, ^3J = 5.4 Hz); 9.13 (s, 2H, $H_{3'}$+$H_{5'}$ PAu-tpy); 8.68 (d, 2H, H_2, ^3J = 8.2 Hz); 8.66 (s, 2H, $H_{3'}$+$H_{5'}$ Ar-tpy); 8.63 (d, 2H, H_3 PAu-tpy, ^3J = 8.3 Hz); 8.49 (d, 2H, H_1, ^3J = 8.1 Hz); 8.43 (d, 2H, H_3 Ar-tpy, ^3J = 7.9 Hz); 8.08 (d, 4H, H_o, ^4J = 1.7 Hz); 8.06 (d, 2H, $H_{o'}$, ^4J = 1.6 Hz); 8.01 (d, 2H, H_4 PAu-tpy, ^3J = 7.3 Hz); 7.98 (d, 2H, H_4 Ar-tpy, ^3J = 7.7 Hz); 7.95 (t, 3H, H_p+$H_{p'}$, ^4J = 1.6 Hz); 7.88 (d, 2H, $H_{o''}$, ^4J = 1.6 Hz); 7.82 (d, 2H, H_6 PAu-tpy, ^3J = 5.4 Hz); 7.76 (d, 2H, H_6 Ar-tpy, ^3J = 5.4 Hz); 7.59 (s, 1H, $H_{p''}$); 7.54 (dd, 2H, H_5 PAu-tpy, ^3J = 6.7 Hz); 7.46 (dd, 2H, H_5 Ar-tpy, ^3J = 6.7 Hz); 1.55 (s, 72H, ^{t}Bu). A nonambiguous attribution could be established on the basis of a 400 MHz ROESY spectrum. MS (FAB$^+$), *m*/*z*: 2425.9 ([M-PF_6]$^+$), 2280.9 ([M-2PF_6]$^+$), 2135.9 ([M-3PF_6]$^+$), 1988.9 ([M-4PF_6]$^+$), 1377.2 ([M-Ir(Artpy)-4PF_6]+, 100%), 1068.6 ([M-3PF_6]$^{2+}$), 994.9 ([M-4PF_6]$^{2+}$).

10. 1 (40 mg, 0.034 mmol) was dissolved in hot absolute ethanol (25 mL). $IrCl_3$·4H_2O (18 mg, 0.048 mmol) in absolute ethanol (15 mL) was then added dropwise, and this mixture was refluxed in the dark for 2h30. The green crude mixture was washed with 5% aqueous Na_2CO_3, which caused a red product to precipitate. It was filtered, dissolved in CH_2Cl_2 and chromatographed twice on alumina (CH_2Cl_2/EtOH: 100/0 to 98/2 and 100/0 to 99/1, respectively) to give **10** in a 58% yield (29.5 mg, 0.020 mmol) as a red-brown solid. ^{1}H NMR (400 MHz, $CDCl_3$), δ (ppm): 9.67 (d, 2H, H_6, ^3J = 5.6 Hz); 8.96 (d, 2H, pyrroles, ^3J = 4.8 Hz); 8.93 (s, 4H, pyrroles); 8.88 (d, 2H, pyrroles, ^3J = 4.8 Hz); 8.58 (s, 2H, $H_{3'}$+$H_{5'}$); 8.51 (d, 2H, H_3, ^3J = 8 Hz); 8.31 (d, 2H, H_2, ^3J = 8 Hz); 8.16 (d, 2H, H_1, ^3J = 8 Hz); 8.10 (d, 4H, H_o, ^4J = 1.6 Hz); 8.08 (d, 2H, $H_{o'}$, ^4J = 1.6 Hz); 8.01 (ddd, 2H, H_4, ^3J = 7.9 Hz, ^4J = 1.8 Hz); 7.81 (m, 3H, H_p+$H_{p'}$); 7.76 (ddd, 2H, H_5, ^3J = 6.5 Hz, ^4J = 1.7 Hz); 1.58 (s, 54H, ^{t}Bu); −2.65 (broad s, 2H, NH). MS (FAB$^+$), *m*/*z*: 1481.8 ([M]$^+$), 1444.8 ([M-Cl]$^+$), 1410.1 ([M-2Cl]$^+$), 1375.2 ([M-3Cl]$^+$), 1182.9 ([M-3Cl-Ir]$^+$).

4^{3+} **(PH_2−Ir).** **10** (40 mg, 0.027 mmol) and Ar-tpy (12 mg, 0.028 mmol) were heated to reflux in degassed ethylene glycol (10 mL), under Ar and in the dark, for 25 min. After cooling to RT, 0.2M aqueous KPF_6 was added (10 mL) to precipitate a dark brown solid, which was subsequently filtered off. After chromatography on alumina (CH_2Cl_2/EtOH: 100/0 to 97/3), 27 mg of pure dyad were obtained (after anion exchange with KPF_6). The impure red-brown fraction was subjected to chromatography on silica (acetone/water/saturated aqueous KNO_3 solution: 100/0/0 to 100/10/0.4) and anion exchange yielded an additional 13 mg of pure $\mathbf{4}^{3+}$ (66% overall yield, 0.018 mmol) as a red-brown solid. ^{1}H NMR (400 MHz, CD_3CN), δ (ppm): 9.45 (s, 2H, $H_{3'}$+$H_{5'}$); 9.08 (s, 2H, $H_{3'}$+$H_{5'}$ Ar-tpy); 8.99−8.97 (m, 4H, pyrroles); 8.90 (s, 4H, pyrroles); 8.89 (d, 2H, H_3, ^3J = 7.7 Hz); 8.84 (d, 2H, H_3 Ar-tpy), ^3J = 7.8 Hz); 8.72−8.68 (m, 4H, H_1+H_2); 8.34−8.27 (m, 4H, H_4); 8.16 (d, 4H, H_o, ^4J = 1.9 Hz); 8.13 (d, 2H, $H_{o'}$, ^4J = 1.7 Hz); 8.02 (d, 2H, $H_{o''}$, ^4J = 1.9 Hz); 7.97−7.94 (m, 3H, H_p+$H_{p'}$); 7.89 (t, 1H, $H_{p''}$, ^4J = 1.7 Hz); 7.84 (dd, 2H, H_6, ^3J = 5.5 Hz, ^4J = 0.8 Hz); 7.77 (dd, 2H, H_6 Ar-tpy), ^3J = 5.8 Hz, ^4J = 0.8 Hz); 7.61−7.54 (m, 4H, H_5); 1.56 (s, 36H, ^{t}Bu); 1.55 (s, 18H, ^{t}Bu′); 1.54 (s, 18H, ^{t}Bu″); −2.71 (broad s, 2H, NH). MS (FAB$^+$), *m*/*z*: 2231.8 ([M]$^+$), 2085.8 ([M-PF_6]$^+$), 1940.8 ([M-2PF_6]$^+$), 1795.9 ([M-3PF_6]$^+$), 1374.7 ([M-3PF_6–Ar-tpy]$^+$), 1182.7 ([M-3PF_6-Ir-Ar-tpy]$^+$), 1043.5 ([M-PF_6]$^{2+}$), 970.9 ([M-2PF_6]$^{2+}$), 898.5 ([M-3PF_6]$^{2+}$), 598.2 ([M-3PF_6]$^{3+}$), 422.3 ([Ar-tpy]$^+$).

6^{4+} **(PH_2−Ir−PAu).** Compound **10** (59 mg, 0.040 mmol) and $\mathbf{2}^+$ (55 mg, 0.036 mmol) were heated to reflux in degassed ethylene glycol (30 mL), under Ar and in the dark, for 25 min. After cooling, precipitation by addition of 0.2M aqueous KPF_6 (30 mL), and filtration of the precipitate, the crude mixture was purified by chromatography on alumina (CH_2Cl_2/EtOH from 100/0 to 50/50) and on silica (acetone/water/saturated aqueous KNO_3 solution from 100/0/0 to 100/10/0.3) to give pure $\mathbf{6}^{4+}$ in a 33% yield (39 mg, 0.012 mmol) as a red-brown solid. The bis-gold analogue **PAu−Ir−PAu** was isolated in 8% yield (10 mg, 0.003 mmol). About 1% PH_2−tpy was also formed by decoordination of the iridium(III), and 10% of both starting materials were recovered after chromatography. ^{1}H NMR ($\mathbf{6}^{4+}$) (400 MHz, CD_3CN), δ (ppm): 9.51−9.45 (m, 8H, PAu-pyrroles); 9.39 (s, 4H, $H_{3'}$+$H_{5'}$); 9.02 (m, 4H, PH_2-pyrroles); 8.96 (d, 4H, H_6+$H_{6''}$, ^3J = 8.2 Hz); 8.93 (s, 4H, PH_2-pyrroles); 8.83−8.73 (m, 8H, H_1+H_2); 8.39 (dd, 4H, H_4+$H_{4''}$, ^3J = 7.8 Hz); 8.21 (d, 4H, PAu−H_o, ^4J = 1.8 Hz); 8.20 (d, 4H, PH_2−H_o, ^4J = 1.8 Hz); 8.19 (d, 2H, PAu−$H_{o'}$, ^4J = 1.8 Hz); 8.16 (d, 2H, PH_2−$H_{o'}$, ^4J = 1.7 Hz); 8.12−8.10 (m, 3H, PAu−H_p+$H_{p'}$); 8.00−7.98 (m, 3H, PH_2−H_p+$H_{p'}$); 7.96−7.92 (m, 4H, H_3+$H_{3''}$); 7.70−7.65 (m, 4H, H_5+$H_{5''}$); 1.60 (s, 36H, PAu-^{t}Bu); 1.59 (s, 18H, PAu-^{t}Bu′); 1.58 (s, 36H, PH_2-^{t}Bu); 1.57 (s, 18H, PH_2-^{t}Bu′); −2.67 (broad s, 2H, NH). MS (FAB$^+$), *m*/*z*: 3187.4 ([M-PF_6+H]$^+$), 3042.4 ([M-2PF_6+H]$^+$), 2896.4 ([M-3PF_6]$^+$), 2751.4 ([M-4PF_6]$^+$). ^{1}H NMR (**PAu−Ir−PAu**) (400 MHz, CD_3CN, 60 °C), δ (ppm): 9.41 (s, 4H, $H_{3'}$+$H_{5'}$); 9.38 (d, 4H, pyrroles, ^3J = 4.8 Hz); 9.35 (d, 4H, pyrroles, ^3J = 4.8 Hz); 9.28 (s, 8H, pyrroles); 8.89 (d, 4H, H_6+$H_{6''}$, ^3J = 7.7 Hz); 8.73 (d, 4H, H_1, ^3J = 7.5 Hz); 8.63 (d, 4H, H_2, ^3J = 7.5 Hz); 8.30 (dd, 4H, H_4+$H_{4''}$, ^3J = 7.7 Hz); 8.11 (d, 8H, H_o, ^4J = 2.0 Hz); 8.08 (d, 4H, $H_{o'}$, ^4J = 2.0 Hz); 8.00 (m, 6H, H_p+$H_{p'}$); 7.87 (d, 4H, H_3+$H_{3''}$, ^3J = 6.7 Hz); 7.61 (m, 4H, H_5+$H_{5''}$); 1.51 (s, 108H, ^{t}Bu).

5^{3+} **(PZn−Ir).** Compound $\mathbf{4}^{3+}$ (24 mg, 0.011 mmol) was refluxed with $Zn(OAc)_2$·2H_2O (4 equiv, 10 mg, 0.044 mmol) in absolute MeOH (10 mL)/MeCN (15 mL) under argon and in the dark for 3 h (the metalation process was monitored by UV−Vis absorption spectroscopy). The crude mixture was purified by chromatography on silica (acetone/water/saturated aqueous KNO_3 solution from 100/0/0 to 100/10/0.3) to give pure $\mathbf{5}^{3+}$ as a red-brown solid in 80% yield (20 mg, 0.009 mmol). ^{1}H NMR (400 MHz, CD_3CN), δ (ppm): 9.45 (s, 2H, $H_{3'}$+$H_{5'}$); 9.08 (s, 2H, $H_{3'}$+$H_{5'}$ ^{t}Buterpy); 8.97 (AB quartet, 4H, pyrroles, ^3J = 4.7 Hz); 8.89 (m, 6H, pyrroles+H_3); 8.83 (d, 2H, H_3 ^{t}Buterpy, ^3J = 7.5 Hz); 8.68 (m, 4H, H_1+H_2); 8.30 (m, 4H, H_4+H_4 ^{t}Buterpy); 8.13 (d, 4H, H_o, ^4J = 1.6 Hz); 8.10 (2H, d, 2H, $H_{o'}$, ^4J = 1.9 Hz); 8.01 (d, 2H, H_o ^{t}Buterpy, ^4J = 1.8 Hz); 7.93 (m, 3H, H_p+$H_{p'}$); 7.88 (t, 1H, H_p ^{t}Buterpy, ^4J = 1.6 Hz); 7.85 (d, 2H, H_6, ^3J = 4.8 Hz); 7.77 (d, 2H, H_6 ^{t}Buterpy, ^3J = 5.0 Hz); 7.58 (m, 4H, H_5+H_5 ^{t}Buterpy); 1.56 (s, 36H, ^{t}Bu); 1.55 (s, 36H, ^{t}Bu). MS (FAB$^+$), *m*/*z*: 2294.3 ([M]$^+$), 2150.4 ([M-PF_6]$^+$), 2004.3 ([M-2PF_6]$^+$), 1858.1 ([M-3PF_6]$^+$), 1074.4 ([M-PF_6]$^{2+}$), 1002.4 ([M-2PF_6]$^{2+}$), 929.4 ([M-3PF_6]$^{2+}$).

7^{4+} **(PZn−Ir−PAu).** Compound $\mathbf{6}^{3+}$ (15 mg, 0.0045 mmol) was refluxed with $Zn(OAc)_2$·2H_2O (4 equiv, 4 mg, 0.018 mmol) in absolute MeOH (3 mL)/MeCN (3 mL) under argon and in the dark for 2 h (the metalation process was monitored by UV−Vis absorption spectroscopy). The crude mixture was purified by chromatography on silica (acetone/water/saturated aqueous KNO_3 solution from 100/0/0 to 100/10/0.3) to give pure $\mathbf{7}^{4+}$ as a red-brown solid in nearly quantitative yield (15 mg, 0.0044 mmol).

^{1}H NMR (400 MHz, CD_3CN) δ (ppm): 9.49−9.42 (m, 8H, pyrroles-PAu); 9.37 (s, 4H, $H_{3'}$+$H_{5'}$); 8.99 (m, 4H, pyrroles-PZn); 8.93 (d, 4H, H_6, ^3J = 8.2 Hz); 8.90 (s, 4H, pyrroles-PZn); 8.80−8.70 (m, 8H, H_1+H_2); 8.36 (dd, 4H, H_4, ^3J = 7.8 Hz); 8.18 (d, 4H, H_o-PAu, ^4J = 1.7 Hz); 8.16 (d, 2H, $H_{o'}$-PAu, ^4J = 1.7 Hz); 8.15 (d, 4H, H_o-PZn, ^4J = 2.0 Hz); 8.11 (d, 2H, $H_{o'}$-PZn, ^4J = 1.9 Hz); 8.09−8.06 (m, 3H, H_p+$H_{p'}$-PAu); 7.95−7.90 (m, 7H, H_p+$H_{p'}$-PZn+H_3); 7.68−7.62 (m, 4H, H_5); 1.58 (s, 36H, ^{t}Bu-PAu); 1.57 (s, 36H, ^{t}Bu-PZn); 1.56 (s, 18H, ^{t}Bu′-PAu); 1.55 (s, 18H, ^{t}Bu′-PZn). MS (FAB$^+$), *m*/*z*: 3249.3 ([M+H−PF_6]$^+$), 3105.2 ([M-2PF_6]$^+$), 2960.2 ([M-3PF_6]$^+$), 2813.1 ([M-4PF_6]$^+$), 1552.1 ([M-2PF_6]$^{2+}$), 1479.1 ([M-3PF_6]$^{2+}$), 1408.1 ([M-4PF_6]$^{2+}$), 1376.1 ([M-4PF_6−Zn+3H-terpyPAu]$^+$, ie [PH_3−Ph-terpy-Ir]$^+$, 100%).

Acknowledgment. We thank the French CNRS and the Italian CNR for financial support. We thank European Commission COST program D11/0004/98 and the French Ministry of Education, Research and Technology for a fellowship to I.M.D. We are also grateful to Johnson Matthey for a generous loan of $IrCl_3$.

Supporting Information Available: Fluorescence spectra and time-resolved luminescence of **PH_2** and **PH_2−Ir−PAu** in acetonitrile and butyronitrile; fluorescence spectra of **PZn** and of **PZn−Ir−PAu** in dichloromethane and toluene; schematic energy level diagram of **PZn−Ir** and **PAu−Ir** in dichloromethane. This material is available free of charge via the Internet at http://pubs.acs.org.

IC010416T